Electronic Supplementary Information

Chemical Modification of Temoporfin - A Second Generation Photosensitizer Activated Using Upconverting Nanoparticles for Singlet Oxygen Generation

Q. Yu,[a] E. M. Rodriguez, [a] R. Naccache, [a] P. Forgione, [a] G. Lamoureux, [a] F. Sanz-Rodriguez,[b] D. Scheglmann[c] and J. A. Capobianco *[a]

[a] Department of Chemistry and Biochemistry, Concordia University, Montreal, Canada, E-mail: John.Capobianco@concordia.ca.
[b] Departamento de Biologia, Facultad de Ciencias, Universidad Autonoma de Madrid, Spain.
[c] Research and Development, Biolitec AG, Germany.

Full reference 25 for Gaussian 09

M. J. Frisch, G. W. Trucks, H. B. Schlegel, G. E. Scuseria, M. A. Robb, J. R. Cheeseman, G. Scalmani, V. Barone, B. Mennucci, G. A. Petersson, H. Nakatsuji, M. Cari-cato, X. Li, H. P. Hratchian, A. F. Izmaylov, J. Bloino, G. Zheng, J. L. Sonnenberg, M. Hada, M. Ehara, K. Toyota, R. Fukuda, J. Hasegawa, M. Ishida, T. Nakajima, Y. Honda, O. Kitao, H. Nakai, T. Vreven, J. A. Jr. Montgomery, J. E. Peralta, F. Ogliaro, M. Bearpark, J. J. Heyd, E. Brothers, K. N. Kudin, V. N. Staroverov, R. Kobayashi, J. Normand, K. Raghavachari, A. Rendell, J. C.Burant, S. S. Iyengar, J. Tomasi, M. Cossi, N. Rega, N. J. Millam, M. Klene, J. E. Knox,J. B. Cross, V. Bakken, C. Adamo,J. Jaramillo, R. Gomperts, R. E. Stratmann, O. Yazyev, A. J. Austin, R. Cammi, C. Pomelli, J. W. Ochterski, R. L. Martin, K. Morokuma, V. G. Zakrzewski, G. A. Voth, P. Salvador, J. J. Dannenberg, S. Dapprich, A. D. Daniels, Ö. Farkas, J. B. Foresman, J. V. Ortiz, J. Cioslowski and D. J. Fox, Gaussian 09, Revision **B.01**; Gaussian, Inc.; Wallingford, CT, 2009.

Table of Contents

1. Experimental Section

Temoporfin was provided by Bioletic AG, Jena, Germany as a powder and all required solutions were prepared in an ethanol/propylene glycol mixture (approved solvents for the administration of Temoporfin).

1.1 Synthesis of $LiYF_4$: Tm^{3+}/Yb^{3+}-UCNPs.

The colloidal upconverting $LiYF_4$: Tm^{3+} 0.5 mol%/Yb^{3+} 25 mol% nanoparticles were synthesized *via* a thermal decomposition method established by our group.[1] All the chemicals utilized during the synthesis were purchased from Alfa Aesar and were used without further purification. Two steps involved in the synthesis are the preparation of the trifluroacetate lanthanide precursors and the formation of ligand-capped nanoparticles. The lanthanide precursors were prepared by dissolving 210.3 mg (0.931 mmol) of yttrium oxide, 123.2 mg (0.313 mmol) of ytterbium oxide and 2.4 mg (0.00625 mmol) of thulium oxide in a mixture of 5 mL of trifluoroacetic acid and 5 mL of water. The reaction mixture was heated to 80 °C under reflux for 12 hours and then slowly evaporated to dryness at 60 °C. A second solution (solution A) containing 12.5 mL of oleic acid and 12.5 mL of 1-octadecene was degassed at 150 °C for 30 min. 299.9 mg (2.5 mmol) of CF_3COOLi was added to the lanthanide precursor and then dissolved in 7.5 mL of oleic acid and 7.5 mL of 1-octadence (solution B). Solution B was slowly heated to 125 ^{0}C under vacuum and solution A was heated to 315 °C under a gentle flow of argon gas. Solution B was transferred into solution A via a syringe and pump system at a rate of 1.5 mL/min. The combined solution was heated under argon at 315 °C for 90 min with continuous stirring. The solution was allowed to cool to room temperature. Ethanol was used to precipitate out the nanoparticles. Nanoparticles were isolated by centrifugation at 4000 rpm (equal to relative centrifugal force of 1350 g) for 15 min and then washed with ethanol/hexane (4:1) mixture twice.

The nanoparticles prepared are capped with oleate ligand on the surface and are hydrophobic. To render the nanoparticles hydrophilic and water dispersible, the capping oleate was removed *via* an HCl treatment.[2] An HCl solution of pH 4 was added to the nanoparticles and stirred vigorously for 2 hours. During this process the oleate was protonated producing oleic acid, the hydrophobic oleic acid was extracted using ethyl ether and removed together with organic layer. The resulting hydrophilic nanoparticles were precipitated using acetone and isolated by centrifugation.

1.2 Addition of linker molecule to m-THPC

4-(Bromomethyl)benzoic acid, 97% purchased from Alfa Aesar, was utilized as a linker to bond m-THPC to the nanoparticles. A sodium hydride suspension in 10 mL of tetrahydrofuran was added to 20 mg (0.029 mmol) of m-THPC. The reaction mixture was heated under reflux for 30 min with stirring. 24.9 mg (0.060 mmol) of 4-(bromomethyl)benzoic acid was added dropwise and the reaction was refluxed for 12 hours. After cooling to room temperature water was added to the mixture and THF was removed under vacuum. The aqueous solution was adjusted to pH 2 using HCl at 5 ^{o}C and the precipitate 5,10,15-tris(m-hydroxyphenyl)-chlorin-20-methyl benzoic acid (m-THPC-MBA) was recovered.

1.3 Surface modification of UCNPs with m-THPC-MBA

Typically, 10 mg of oleate-free UCNPs were dispersed in 4 mL of water followed by the addition of 1 mg of m-THPC-MBA in 1 mL of ethanol. The mixture was adjusted to a neutral pH to deprotonate the carboxylic group on the m-THPC-MBA and stirred for 6 days at room temperature. The modified UCNPs were precipitated in acetone and then isolated by centrifugation at 4000 rpm for 15 minutes m-THPC-MBA dissolves in acetone and was removed with the supernatant.

1.4 Determination of concentration of m-THCP-MBA on the nanoconstruct

The concentration of m-THPC-MBA on the surface of the $LiYF_4:Tm^{3+}/Yb^{3+}$-UCNPs was determined by measuring the absorbance of m-THPC-MBA-$LiYF_4:Tm^{3+}/Yb^{3+}$-UCNPs at 438 nm. Using this absorbance value and its absorption coefficient obtained from the calibration curve of m-THPC-MBA we found the concentration of m-THPC-MBA on the nanoparticles to be 4.8×10^{-5} M, which represents approximately 7.6×10^3 molecules of m-THPC-MBA on the surface of the UCNPs.

1.5 Detection of singlet oxygen

The singlet oxygen generated by the m-THPC-MBA-$LiYF_4:Tm^{3+}/Yb^{3+}$-UCNPs irradiated at 980 nm was monitored using the chemical trap 1, 3-diphenylisobenzofuran (DPBF). All the measurements were performed in air-saturated propylene glycol/ethanol solution in a 10 mm x 10 mm quartz cuvette. The total volume of solution used was 2 mL and a concentration of 2.5×10^{-5} M of DPBF. Concentration of m-THPC-MBA-$LiYF_4:Tm^{3+}/Yb^{3+}$-UCNPs is 1 mg/mL which is equal to 5×10^{-5} M of m-THPC-MBA in solution.

1.6 Cell viability tests showing the applicability of nanoconstruct in photodynamic therapy

Cell viability of HeLa cells exposed to the m-THPC-MBA-$LiYF_4:Tm^{3+}/Yb^{3+}$-UCNPs and to NIR light was analyzed by the MTT (3-[4,5-dimethylthiazol-2-yl]-2,5-diphenyltetrazoliumbromide) colorimetric assay.[3] This method is based on the capacity of living cells which possess dehydrogenases to reduce the salt of tretazolio MTT to a colored and insoluble compound, formazan.

In the first experiment HeLa cells were incubated for 4 h with the m-THPC-MBA-$LiYF_4:Tm^{3+}/Yb^{3+}$-UCNPs. After that, the cells were incubated with MTT (0.1 mg/ml in DMEM with 10% SFB and 1% L-glutamine) during 4 hours at 37 °C. Then the medium with the MTT

was removed and crystallized formazan was suspended with 1 ml of dimethylsulphoxide (DMSO). Immediately after, we proceeded to measure the absorbance at 540 nm using a plate reader (Espectra Fluor 4, Tecan). Cell viability was estimated as a percentage relative (100% viability) to the mean of the absorption obtained from the control cells (not incubated with nanoparticles).

In the second experiment, following a four hour incubation with the -m-THPC-MBA-UCNP nanoparticles, the cells were exposed to NIR irradiation for 1 hour (using Hydrosun®750 source).

1.7 Computational calculations of the electronic absorption spectra of m-THPC and m-THPC-MBA with linker at different positions

All the calculations were carried out using Gaussian 09 software package provided by the Golem Server at Concordia University.

The time-dependent density functional theory was combined with Becke Three Parameter Hybrid Functionals (B3LYP) and the basis set 6-31G(d,p) was used to optimize the ground state geometry of the m-THPC and m-THPC-MBA.[4,5] The solvent effect (ethanol) was simulated using the conductor-like polarizable continuum model (CPCM).[6,7] The models used, m-THPC-MBA (I), m-THPC-MBA (II), m-THPC-MBA (III), shown in Scheme S1, are based on the possible reactive sites of m-THPC. The ground-state geometry of m-THPC and the three models were optimized and the optimized geometries were verified to be local minima by frequency calculations.

2. Characterization

2.1 Fourier Transform Infrared (FTIR) Spectroscopy

FTIR spectra of the as-synthesized oleate-capped $LiYF_4$: Tm^{3+}/Yb^{3+}-UCNPs, and the oleate-free $LiYF_4$: Tm^{3+}/Yb^{3+}-UCNPs were measured on a Nicolet 6700 FTIR spectrometer using the KBr pellet.

2.2 Transmission Electron Microscopy (TEM)

TEM analysis of the colloidal dispersion of $LiYF_4$: Tm^{3+}/Yb^{3+}-UCNPs was performed using a Philips CM200 microscope operating at 200 kV equipped with a charge-coupled device (CCD) camera (Gatan). Prior to analysis, the sample was dispersed in toluene to yield an approximate 0.5 wt% solution. A few drops of the resulting solution were evaporated on a formvar/carbon film supported on a 300 mesh copper grid (3 mm in diameter).

2.3 X-Ray Powder Diffraction (XRPD)

XRPD patterns were measured using a Scintag XDS-2000 Diffractometer equipped with a Si(Li) Peltier-cooled solid state detector, Cu Kα source at a generator power of 45 kV and 40 mA, divergent beam (2 mm and 4 mm), and receiving beam slits (0.5 mm and 0.2 mm). The scan range was set from 20-80° 2θ with a step size of 0.02° and a count time of 2 s. The sample was measured using a quartz "zero background" disk.

2.4 Upconversion Luminescence Spectroscopy

The upconversion visible emission spectra of the oleate-free $LiYF_4$: Tm^{3+}/Yb^{3+}-UCNPs and the Ln^{3+}-UCNP-m-THCP-MBA were obtained upon 980 nm excitation, using a Coherent 6-pin fiber-coupled F6 series 980 nm laser diode (power of 615 mW), coupled to a 100 μm (core)

fiber. For the upconversion studies, the samples (1 wt% in EtOH/propylene glycol) were placed in 1 cm path-length quartz cuvettes (Hellma, QS). The upconverted visible emissions were collected at right angle with respect to the incident beam and subsequently dispersed by a 1m Jarrell-Ash Czerny-Turner double monochromator with an optical resolution of ~0.15 nm. The emission was detected by a thermoelectrically cooled Hamamatsu R943-02 photomultiplier tube. A preamplifier, model SR440 Standard Research Systems, processed the photomultiplier signals and a gated photon counter model SR400 Standard Research Systems data acquisition system was used as an interface between the computer and the spectroscopic hardware. The signal was recorded under computer control using the Standard Research Systems SR465 software data acquisition/analyzer system.

The UV emission was collected using a SpexMinimate ¼ m monochromator and detected with an Oriel 70680 photomultiplier tube. It should be noted that the UV and visible emissions were measured with different detectors that overlap in the blue region. Thus, by measuring the overlapping regions with both monochromators, under identical conditions, the intensity of the UV emissions could be compared to the visible ones.

2.5 UV/Vis Absorption Measurement

UV/Vis absorption spectra of m-THCP, m-THCP-MBA and Ln^{3+}-UCNP-m-THCP-MBA were all measured in solvent mixture propylene glycol/EtOH and were recorded using Varian (Mulgrave, Victoria, Australia) Cary 5 and 5000 spectrophotometers.

2.6 Mass Spectrometry

Mass spectrometry measurements were performed by a LC-MSD TOF (Agilent) using ESI as the ionisation source with mass range of 50 – 8000m/z.

Preparative Liquid Chromatography – Mass Spectrometry (Prep LC-MS) was applied to separate the two isomers in the product and the reagent m-THPC, using MSQ Plus ™ Single Quadrupole Mass Spectrometer from Thermo Scientific ™.

3. References

1. V. Mahalingam, F. Vetrone, R. Naccache, A. Speghini and J. A. Capobianco, *Adv. Funct. Mater.* 2009, **21**, 4025.
2. N. Bodgan, F. Vetrone, G. Ozin and J. A. Capobianco, *Nano Lett.* 2011, **11**, 835.
3. M. V. Berridge and A. S. Tan, *Arch BiochemBiophys.* 1993, **303**, 474.
4. C. Lee, W. Yang and G. R. Parr, *Phys. Rev. B: Condens. Matter Mater. Phys*. 1988, **37**, 785.
5. A. D. Becke, *J. Chem. Phys*. 1993, **98**, 5648.
6. M. Cossi, N. Rega, G. Scalmani and V. Barone, *J. Comput. Chem.* 2003, **24**, 669.
7. V. Barone and M. Cossi, *J. Phys. Chem. A*. 1998, **102**, 1995.

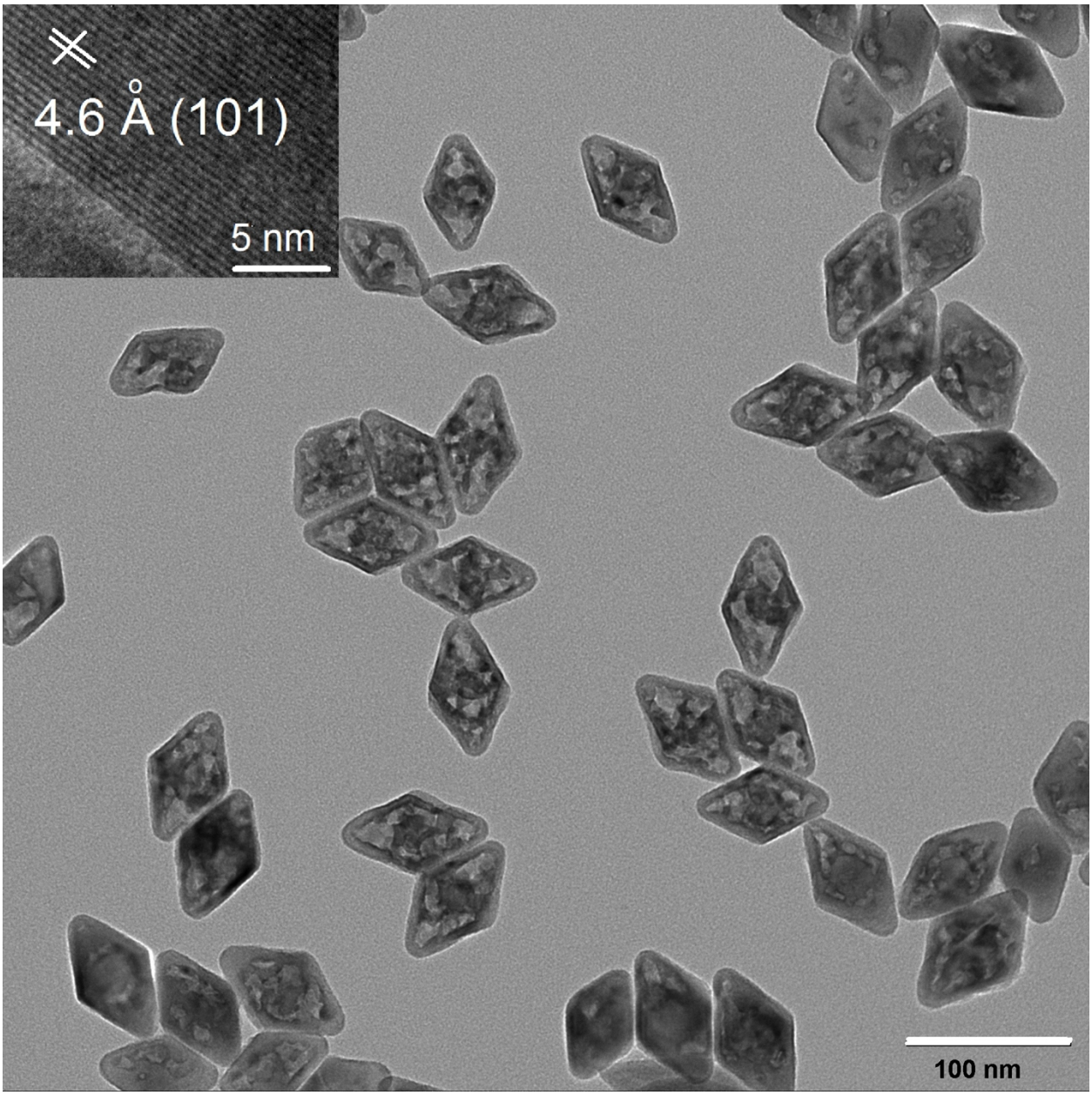

Figure S1. Transmission electron microscopy image of oleate-capped $LiYF_4$: Tm^{3+}/Yb^{3+}-UCNPs (0.5 wt% in toluene). Inset: high resolution TEM image showing the lattice arrangement of the atoms in the crystals. The distance between the adjacent planes (d-spacing) was measured to be 4.6 Å, which is accordance with the (101) planes in $LiYF_4$.

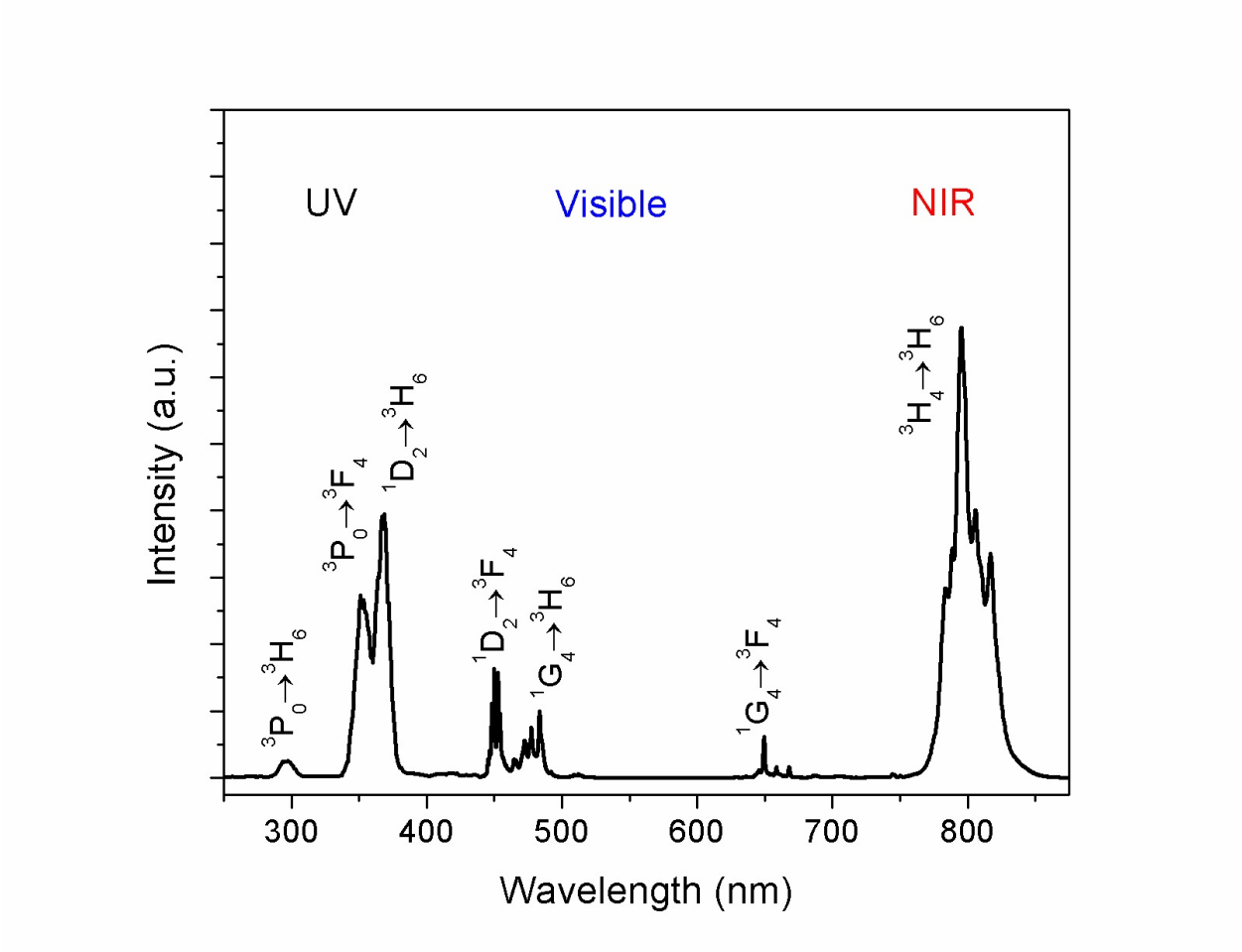

Figure S2. Upconverted luminescence emission spectrum of $LiYF_4$: Tm^{3+}/Yb^{3+}-UCNPs from the UV to NIR regions (0.5 wt% in toluene).

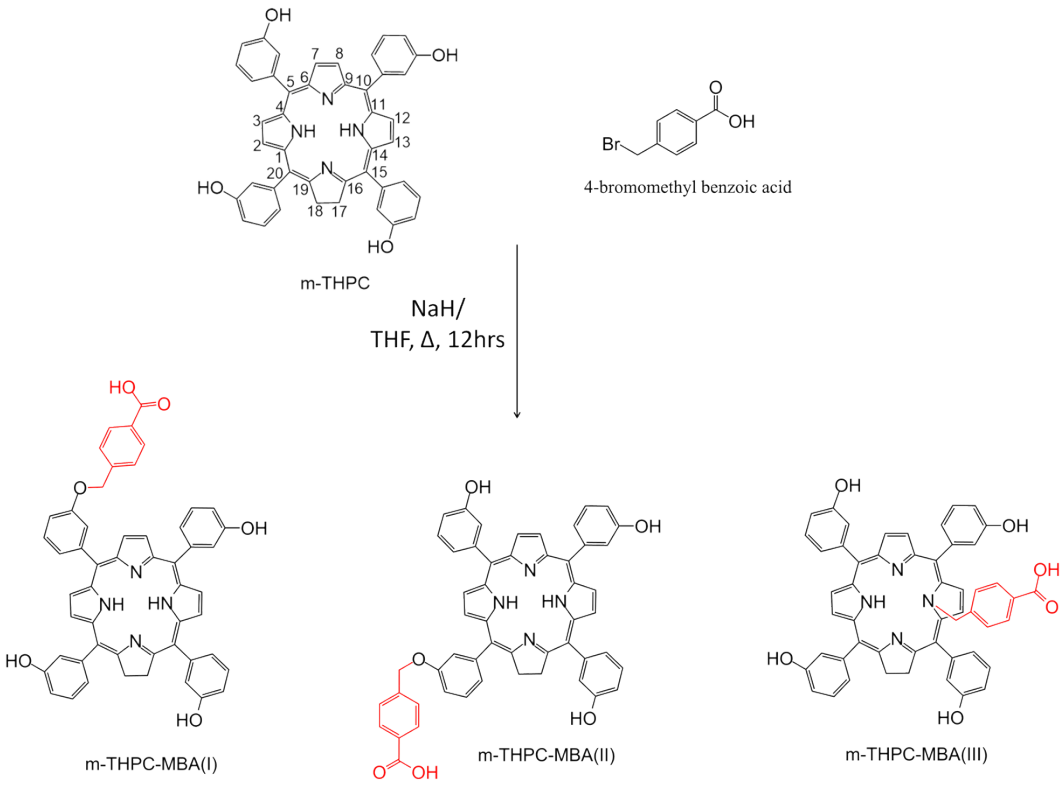

Scheme S1. Conversion of m-THPC to m-THPC-MBA endowing a carboxylic acid functionality to the latter and allowing for the molecule to cap the positively charged nanoparticle surface.

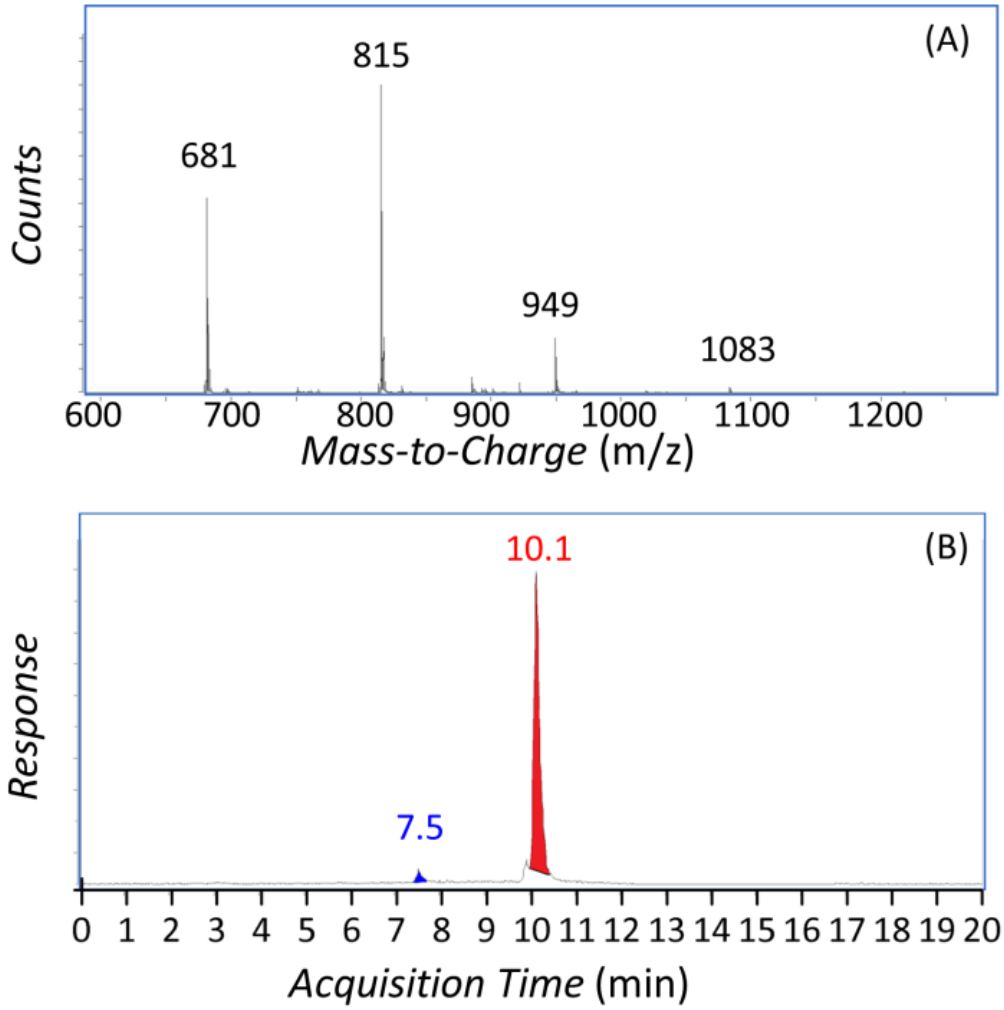

Figure S3. (A) LC-MS of the product from the coupling reaction. The spectrum shows four compounds; (a) m-THPC, (b) m-THPC-MBA with one linker, (c) m-THPC-MBA with 2 linkers and (d) m-THPC-MBA with 3 linkers. **(B)** Elution profile from Prep LC-MS. Isomers m-THPC-MBA (I) and (II) with molecular weight of 815 were eluted at retention time 10.1 min, and isomer m-THPC-MBA (III) was eluted at 7.5 min.

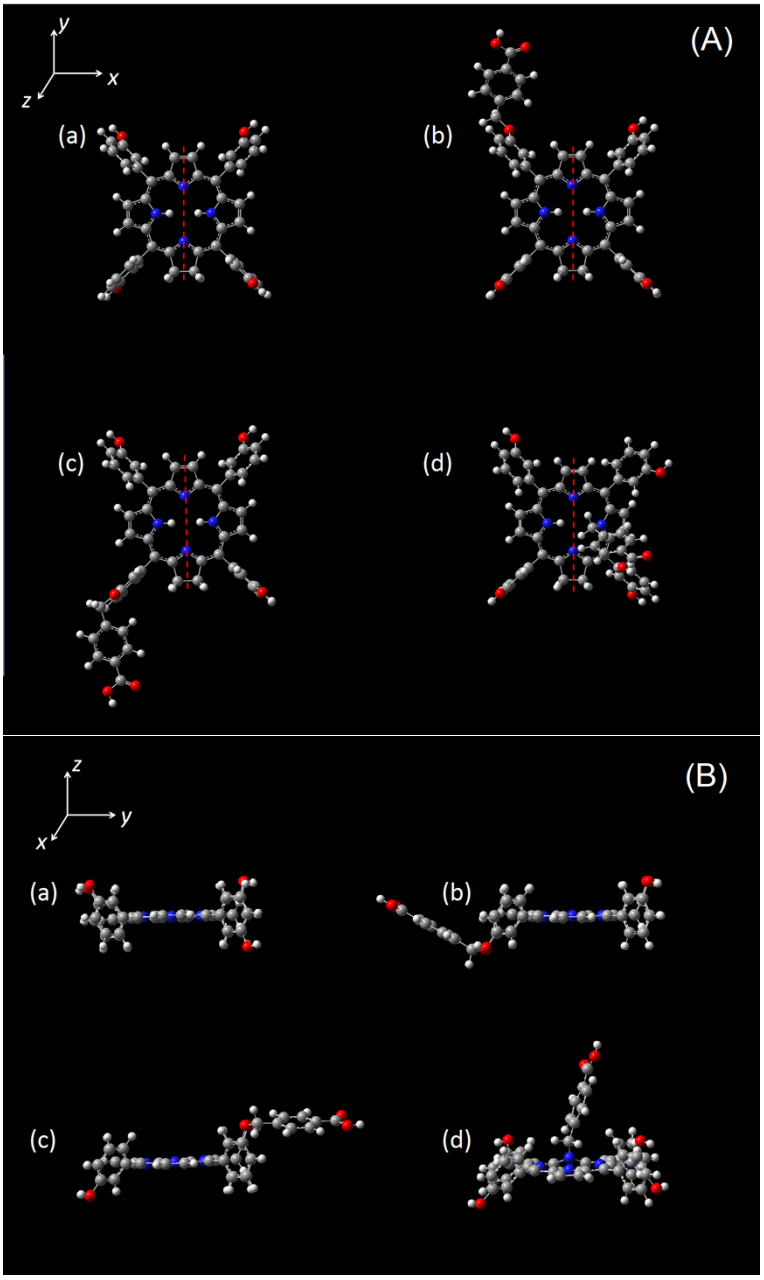

Figure S4. (A) Top view of the ground-state molecular structures of (a) m-THPC, (b) m-THPC-MBA (I), (c) m-THPC-MBA (II), and (d) m-THPC-MBA (III) optimized at the TD-DFT/B3LYP level. The red dash line passing through the two pyrroles (----) represents the yz-plane of symmetry, **(B)** side view, three of the molecules (a, b, c) have a planar chlorin ring while in (d) the chlorin ring is not planar due to the addition of the linker directly onto the ring.

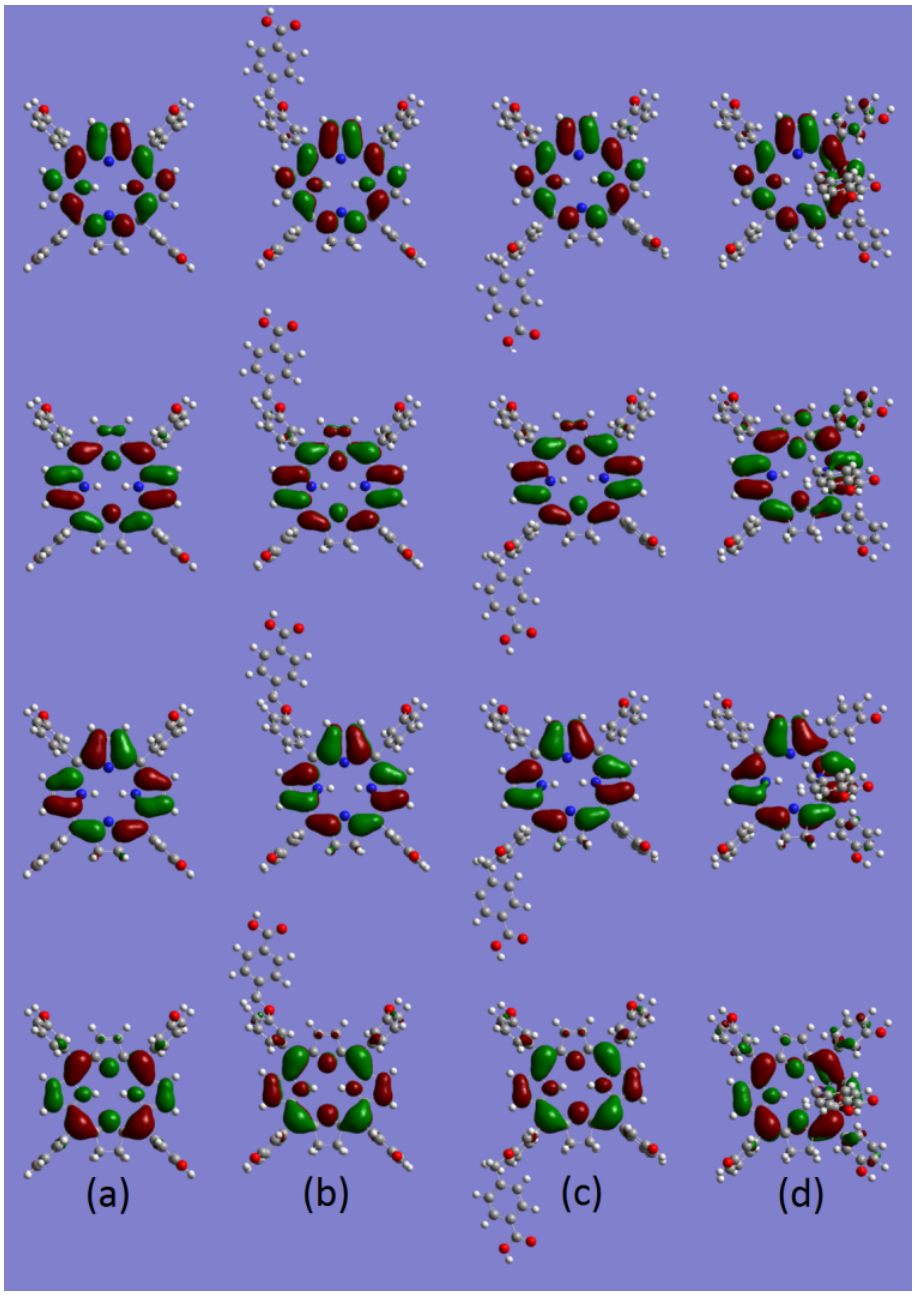

Figure S5. Calculated molecular orbitals (from bottom to top, HOMO -1 through LUMO +1) for m-THPC, m-THPC-MBA (I), m-THPC-MBA (II), and m-THPC-MBA (III), from left to right. The electron density is shown as the balloons in red (positive wavefunction) and green (negative wavefunction). The molecular orbitals of the chlorin ring show no difference in m-THPC, m-THPC-MBA (I), and m-THPC-MBA (II), while in m-THPC-MBA (III) the π-orbitals between carbon 10 and 11 (in HOMO-1) and between carbon 8 and 9 (in HOMO) have a larger volume compared with the three other molecules.

Table S1. Calculated excitation energies and oscillator strengths of m-THPC, m-THPC-MBA (I), m-THPC-MBA (II), and m-THPC-MBA (III) in EtOH using TD-DFT/B3LYP.

State		Wavelength (nm)	Excited Energy (eV)	Oscillator Strength
m-THPC	S_1	572.11	2.1671	0.1360
	S_2	530.75	2.3360	0.0727
	S_3	408.05	3.0384	1.1918
	S_4	398.47	3.1115	1.5092
	T_1	884.86	1.4012	n/a
m-THPC-MBA (I)	S_1	572.66	2.1651	0.1292
	S_2	532.57	2.3280	0.0838
	S_3	409.29	3.0292	1.2229
	S_4	399.56	3.1030	1.5805
	T_1	886.65	1.3984	n/a
m-THPC-MBA (II)	S_1	573.01	2.1637	0.1293
	S_2	533.12	2.3256	0.0853
	S_3	409.83	3.0253	1.2347
	S_4	399.83	3.1009	1.5605
	T_1	887.61	1.3968	n/a
m-THPC-MBA (III)	S_1	593.73	2.0882	0.0937
	S_2	564.90	2.1948	0.1863
	S_3	432.71	2.8653	1.1580
	S_4	417.85	2.9672	1.0851
	T_1	1005.58	1.2330	n/a

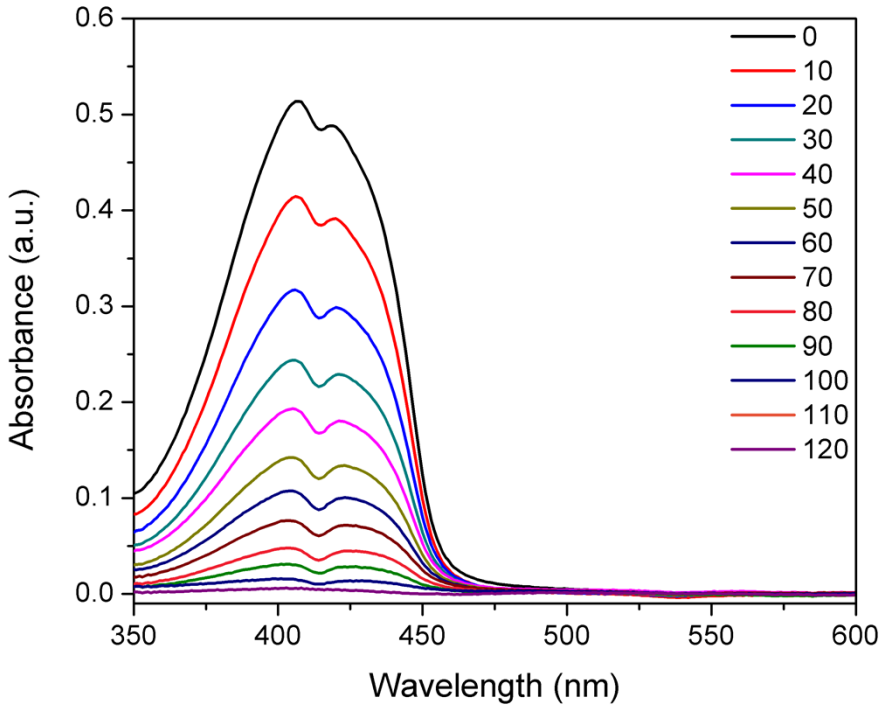

Figure S6. Decrease in the absorption of DPBF in a DPBF (2.5 x 10^{-5} M)/m-THPC-MBA-UCNPs (1 mg/mL) solution as a function of NIR irradiation time (min).